Magnetization processes and reorientation transition for small magnetic dots

R. L. Stamps
Department of Physics, University of Western Australia, Nedlands, WA 6907, Australia

R. E. Camley
Department of Physics, University of Colorado, Colorado Springs, Colorado 80933

(Received 1 December 1998; revised manuscript received 21 June 1999)

A theory for magnetization processes in interacting arrays of small magnetic structures at finite temperatures is presented. Hysteresis and magnetic ordering of weakly coupled arrays of single-domain ferromagnetic particles are examined. The dots are arranged on a planar lattice and the effects of lattice geometry are examined via long-ranged dipolar coupling between magnetic dots. Small clusters of dots arranged in finite arrays are shown to have complicated hysteresis determined by the shape, size, and orientation of the cluster in externally applied fields. One result is an array induced ''shape'' anisotropy that controls how reversal occurs in the array itself. Finite temperature effects are examined and the strength of the dipolar coupling, though weak, can be significant for closely packed particles at low temperatures. A reorientation transition from in plane to perpendicular is shown to occur as the temperature is increased for dots with perpendicular anisotropy. [S0163-1829(99)14635-6]

I. INTRODUCTION

The magnetic properties of single-domain fine particles have been extensively studied, particularly in reference to applications for magnetic recording.[1] Studies of magnetization processes and dynamics in artificially patterned structures has encouraged additional recent efforts and is currently an area of intense interest. The reason is that emerging technology can fabricate independent magnetic wire and dot structures with physical extensions on the submicrometer and nanometer length scale, and so offers a new window on the study of small-particle magnetism.[2,3] The extreme precision with which elements and arrays can be constructed opens many fascinating possibilities for studying and controlling unusual hysteresis processes as well as high-frequency dynamics.[4]

The potential small size and high density of large moment particle arrays mean that energies typically ignored in discussions of conventional fine-particle research can be significant. For example, the dipolar field acting at the center of a cube in a square array of perpendicularly magnetized 0.5 μm-wide Fe cubes is approximately 900 G/cm^3 if the cubes are centered on a 1-μm array. These fields are comparable to bulk cubic anisotropy fields and therefore have the potential to strongly affect static magnetic order and magnetization processes. Dipolar effects on static properties are often neglected in treatments of ensembles of small particles because the fields rapidly become small as the spacing between dots is increased. This is particularly true in a two-dimensional lattice.

Finite arrays of only a few magnetic dots can exhibit stronger dependencies on dipolar fields. This is because a small array of dots can have a large circumference to area ratio, meaning that finite size effects from a truncated *array* can have a large effect on static and dynamic properties.[5] A surprising result is that even very weak coupling between magnetic dots can strongly influence nonlinear dynamic behavior.[6] This has particular relevance to high-speed switching properties[7] and as will be shown here, thermally driven magnetic reorientations.

The paper is organized as follows. In Sec. II, the calculation technique is described and results presented for array size determined hysteresis. In Sec. III, the effects of temperature are discussed and a reorientation transition described. A summary is given in Sec. IV.

II. ARRAY SIZE DETERMINED HYSTERESIS

The basic calculation method is to numerically integrate the time-dependent Landau-Lifshitz equations of motion for an array of interacting magnetic dots. This has an advantage over conventional micromagnetic modeling in that relaxation mechanisms involving precession can be easily taken into account.[5] The same model can also be easily extended to investigate the dynamic properties of the array.

Time integration scheme

The theory described below describes interaction and finite temperature effects for arrays of ferromagnetic dots. The dots interact weakly via dipolar stray fields, and low temperatures are assumed. The dots are presumed to support single domains in all cases considered, so for simplicity, the dots are assumed to be uniformly magnetized. This is a reasonable assumption for the purposes of this paper because the essential features of the magnetic ordering and dynamic response are governed primarily by the net magnetic moment of each particle.

The arrangement of dots is shown schematically in Fig. 1. A dot's position is given by the position **i** in the array corresponding to a position vector $\mathbf{r}_i = \mathbf{x}na + \mathbf{y}ma$ where a is the lattice spacing and n and m are integers. The time-dependent equation of motion of a dot magnetic moment **m** at position **i** in the array is

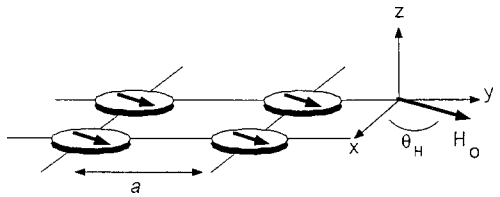

FIG. 1. Geometry of square array of magnetic dots. The dots are small cylinders centered on lattice points of a submicron size array. The position of each dot is measured relative to the dot center on an array of lattice size *a*.

$$d\mathbf{m}_i/dt = \gamma \mathbf{m}_i \times \mathbf{H}_i - \alpha \mathbf{m}_i \times \mathbf{m}_i \times \mathbf{H}_i. \tag{1}$$

Here, γ is the gyromagnetic ratio, and α controls the rate of dissipation. This form of dissipation is chosen to conserve the magnitude of the dot moment as $|\mathbf{m}|/V = M$ where V is the dot volume. The field $\mathbf{H}_i$ is an average effective field acting at position **i**:

$$\mathbf{H}_i = \mathbf{x} H_0 \cos\theta_H + \mathbf{y} H_0 \sin\theta_H + \mathbf{z}[(2K/M^2) m_{zi}] - \mathbf{d}_i. \tag{2}$$

Contributions to $\mathbf{H}_i$ are a static applied field H_0 set an angle θ_H to the x direction in the first two terms, and anisotropy and dipolar fields in the remaining terms.

The shape and magnetocrystalline contributions to the anisotropies in the dots are described by a single uniaxial anisotropy K with easy axis directed normal to the dot array plane, as would be appropriate for cylindrical dots. A time-dependent dipole field $\mathbf{d}_i$ due to all the other dots in the array is included:

$$\mathbf{d}_i = \sum_i \left[\frac{\mathbf{m}_i}{r_i^3} - 3 \frac{\mathbf{r}_i \cdot \mathbf{m}_i}{r_i^5} \mathbf{r}_i \right]. \tag{3}$$

Unitless variables are chosen so that fields and energies are given as ratios relative to M (such as K/M^2) and time is given by the variable $\gamma M t$. The calculation is performed by solving the set of $3N^2$ coupled equations for a square dot array of dimension N numerically using a second-order Runge-Kutta method. In this technique, the time evolution of each dot in the array is calculated over a small time interval Δt. Typically, convergent solutions for static order can be found with Δt on the order of 0.005 within 1000 time steps (in units of $\gamma M t$) for small arrays (N around 4) the precession term is dropped and only the relaxation term is kept in Eq. (1).

As mentioned above, parameters for the calculations are in units reduced by the magnetization of the dot material M. In these unitless variables, the dipolar term is then of the form $d/M \propto V/r^3$. Because of the sum over dipoles in Eq. (3), the dipole strength is determined by the physical structure of the array and the strength is given by the ratio of dot volume to array cell volume. This ratio is denoted as h_d and is given by

$$h_d = \pi h R^2 / a^3, \tag{4}$$

where h and R are the height and radius of a dot cylinder, and a is the center to center distance between nearest neighbor dots. Unless otherwise specified, the dipolar coupling strength is $h_d = 0.5$ for the examples considered in this paper.

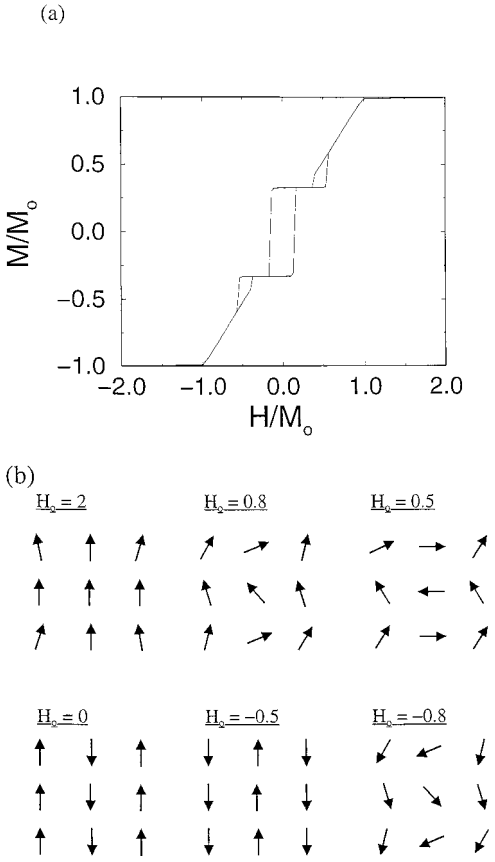

FIG. 2. Magnetization loops for a 3×3 square in-plane magnetized magnetic dot array are shown in (a). The applied field is aligned parallel to an array. The dipolar coupling strength is $h_d = 0.5$. Spin configurations at points along the loop are shown in (b). Reversal takes place first along the middle column of moments.

Field orientation and size effects

Effects of applied field orientation are shown in Fig. 2 for a 3×3 square array of dots magnetized in plane with an easy plane anisotropy of -4π. The average magnetic moment of the dot array in the direction of a static applied field is shown for the applied field aligned parallel to an array edge. In Fig. 3, the same calculation is repeated except that the applied field is aligned along an array diagonal.

In both cases a uniformly magnetized state for the *array* is unstable in the absence of a field. Below the saturation field, the dot moments rotate in order to minimize magnetostatic energies originating from uncompensated magnetic poles at the array edges. Different spin arrangements are possible, and alignment of the magnetic field determines the configuration the dots relax into as the field is reduced. As shown in Figs. 2 and 3, the two different field alignments produce very different hysteresis loops.

The moment orientations in the lattice are sketched in Figs. 2(b) and 3(b). When the field is applied along an array edge, magnetostatic energies are minimized near saturation by slight rotations of the corner moments, as seen in Fig. 2(b) for $H_0 = 2$ M. The effect of the corner moment rotations can be seen in Fig. 2(a) as a very small reduction of the average array moment from complete saturation. When the field is applied along a diagonal, as in Fig. 3(a), the corner moments align with the field whereas the moments at the

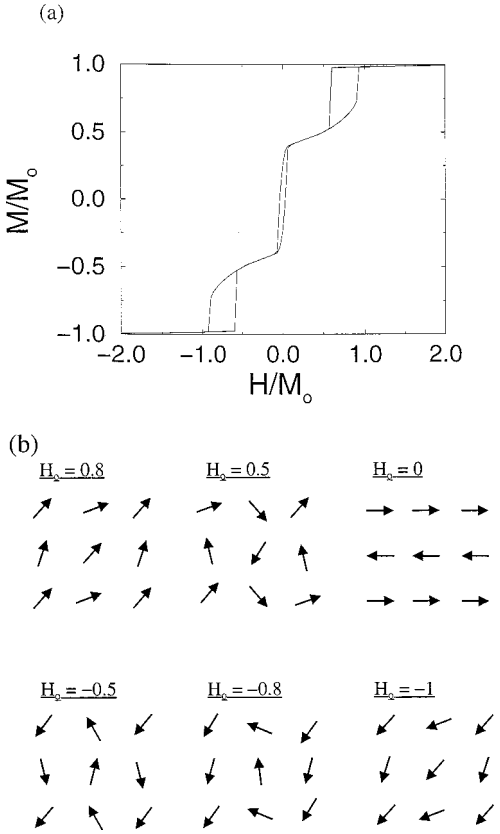

FIG. 3. Magnetization loops for a 3×3 square in-plane magnetized magnetic dot array are shown in (a) with the applied field aligned along an array diagonal. Spin configurations at points along the loop are shown in (b).

side centers rotate. This is depicted for $H_0 = 0.8\,\mathrm{M}$ in Fig. 3(b). A corresponding reduction from saturation is also seen in Fig. 3(a). The net effect of applied field orientation is to provide different initial conditions for the rotation of the array moments as the field is reduced.

In both cases, several of the array moments occur by reversing first the moments of dots along a column of the square array. The zero-field configurations are the same independent of the field orientation with alternating rows or columns of magnetization. This configuration is stable for a range of field values with the field aligned parallel to an array. The configuration is not stable for the field aligned along a diagonal.

The sensitivity of the hysteresis loop to initial conditions requires some care in performing the calculations. Perfect alignment along a high-symmetry direction can result in the appearance of metastable states that disappear for very small misalignments of the applied field. For the reason, the results are shown with the field not directly along an array edge or diagonal, but instead misaligned 0.1° away.

Even or odd N also has a strong effect on the shape of the magnetization loops for small N. Examples are given in Ref. 5, and not repeated here. Instead, it is noted that for small N, there is a great distinction between even N and odd N mainly because in zero field there is a significantly reduced remnant average moment for N even. As N is increased, the distinction between even and odd becomes less pronounced, and minor hysteresis loops are lost.

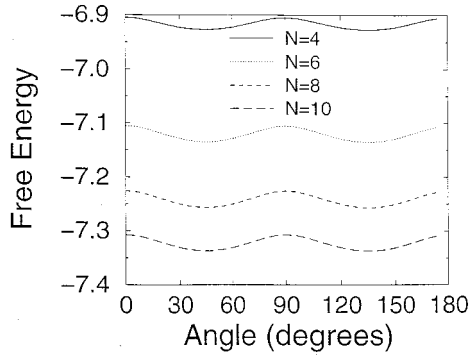

FIG. 4. Energy at $T=0$ for square arrays of in-plane magnetized dots saturated by a large applied field ($H/M_0 = 6$). The energy is calculated for different orientations of the field rotated in the plane of the array. Array shape effects appear in analogy to ferromagnetic shape anisotropies with a symmetry reflecting the symmetry of the square lattice. The overall contribution of magnetostatic energy increases approximately as the ratio of circumference to area.

The geometry of the array creates an orientation dependence of the magnetostatic energy in the saturated state in analogy to ferromagnets. This is a shape anisotropy in the sense that the shape of the dot array determines the symmetry properties of the magnetostatic energy in the array. A square lattice has fourfold symmetry, and this is reflected in the total energy of the dot array calculated as a function of the angle of the applied field θ_H.

The energy is shown in Fig. 4 where the free energy at zero temperature is shown as a function of the size of the lattice. The field is large enough to saturate the sample at $H/M_0 = 6$. The fourfold symmetry of the lattice is evident and is retained as the size of the lattice is increased. The difference between easy and hard directions does not change with increasing N, but the average energy does. The average increases with increasing N, but approaches a limiting value roughly as $1/N$, the ratio of circumference to area.

Array lattice symmetry

The above results illustrate the great sensitivity of dot array magnetization processes to array geometry for the simplest array geometry: a square lattice. Lattice geometry is also important in determining magnetization properties of dot arrays, with distortions from simple square lattices and other lattice symmetries leading to preferred directions of the magnetization and possible frustrations.

Examples of array symmetry effects are given in Fig. 5. In Fig. 5(a), $M(H)$ for a simple square array is contrasted with an equal number of dots in a rhomboid array. The rhomboid has one side 50% longer than the other, and the field is aligned along a long side. $N=3$ for both examples. The rhomboid structure displays a much larger MH product than the square lattice by favoring parallel alignment of dot magnetizations. The sharp drop of the magnetization at $H_0 = -0.4\,\mathrm{M}$ is due to the reversal of a line of moments, reducing the total moment to one third its full value.

In Fig. 5(b), the magnetizations of hexagonal arrays are shown. The dashed line is for a cell of seven dots and the solid line is for the same cell with the center dot removed

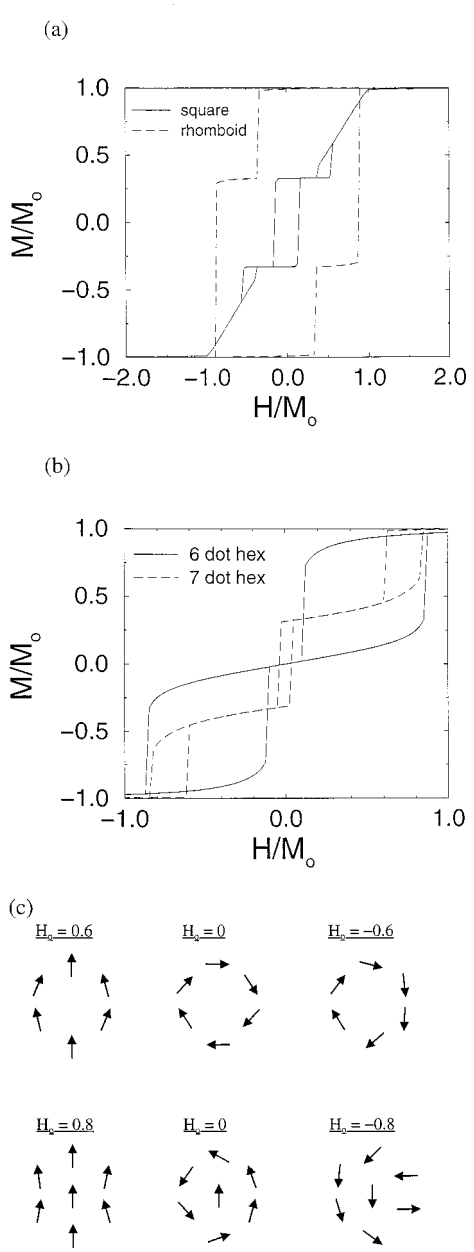

FIG. 5. Array symmetry effects for (a) rhomboid and (b) hexagonal lattices. In (a), $M(H)$ for an $N=3$ array of dots is shown for a rhomboid geometry with the long side 50% longer than the length of the short side. In (b) $M(H)$ is shown for seven dots in a hexagonal pattern by a dashed line. The solid line is $M(H)$ for the same configuration without the center dot. Spin configurations at different points along the loops are shown in (c) for the hexagonal arrays. Hysteresis is due to a reversal process that begins on one side of the array in the hexagonal lattices.

(for a total of six dots). The role of the center dot is important in determining the magnetization process of the array. Sketches of the moment configuration for the two hexagonal arrays are shown in Fig. 5(c). A center dot affects the initial configuration near saturation by deforming the alignment of moments in the hexagonal ring. As reversal develops, the center dot continues to influence the orientation of the ring moments. At zero field, the net moment of the array is enhanced through the center dot moment. The center dot also reduces the size of the minor loops, as seen by comparison of the 6- and 7-dot hysteresis loops.

III. FINITE TEMPERATURES

The previous discussion has considered behavior at zero temperature. The dipolar coupling is weak compared to anisotropy and Zeeman energies, and is strongly affected by thermal fluctuations. An estimate of the temperature above which dipole-induced correlations disappear is twice the interaction energy per dot. This energy is on the order of $2(N-1)(VM)^2/Na^3$ where V is the volume of a dot. For 0.5-μm Fe cubes, this energy is on the order of 10^{-14} erg, which corresponds to a temperature around 200 K. This temperature increases rapidly with particle volume and total magnetic moment, so critical temperatures around room temperature can be readily achieved.

Large thermal fluctuations destroy the hysteresis effects described in Figs. 1 and 2. This can be shown by using a mean-field theory together with the time integration technique. This is done by defining a thermally averaged effective field where all components of **m** appearing in the field defined in Eqs. (2) and (3) are replaced with their mean-field averaged values.[8] Each dot is a large collection of strongly ferromagnetically coupled spins, so all orientations of the total magnetic moment of a dot are possible. The thermal averaged magnetization for each dot at a position i can then be represented by a Langevin function L:

$$\langle m_i\rangle = g\mu_B nJL(nJg\mu_B H_i/k_BT)$$
$$= g\mu_B nJ\left[\coth\left(\frac{nJg\mu_B H_i}{k_BT}\right)-\frac{k_BT}{nJg\mu_B H_i}\right]. \qquad (5)$$

In Eq. (5), the total angular momentum number per atom is J and the number of spins per dot is n, so that $m_i = g\mu_B nJ$ at $T=0$. H_i is the magnitude of the thermal averaged effective field acting on the dot at position i.

Because the effective field H_i is itself a function of the $\langle m_i\rangle$, the time-dependent equations of motion must be solved self-consistently over each interval of time. The method to achieve self-consistency is to begin by assuming a configuration for the m_i, such as saturation with zero-temperature magnitudes at large fields, and then calculate the thermal average $\langle m_i\rangle$ based on this configuration. New values for the m_i are then found for a time Δt later, and new $\langle m_i\rangle$ calculated. The process is continued until equilibrium is reached and the m_i and $\langle m_i\rangle$ no longer change.

This scheme is still valid at finite temperatures as long as adiabatic assumptions apply. This means that the time step must be supposed large compared to the thermal fluctuation time. The moments then have sufficient time during each time step to come into thermal equilibrium. This assumption is enforced by setting $\gamma=0$ in Eq. (1), which implies that the time evolution occurs over time steps sufficiently long that precession effects die out via dissipation of kinetic energy to the lattice. High-frequency transient effects require special consideration and are discussed elsewhere.[6]

Results for temperature effects on hysteresis are shown in Fig. 6. There are nine dots magnetized in the array plane and the field is applied along an array diagonal as in Fig. 2(b). The reduced inverse temperature is $\beta = 1/k_BT$. The effect of

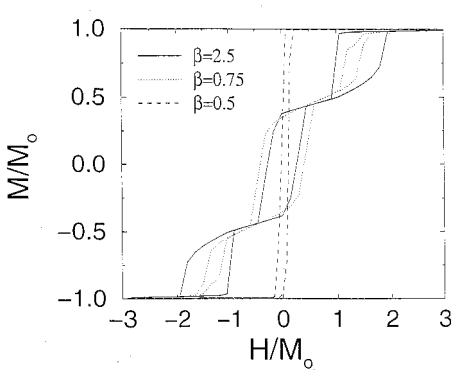

FIG. 6. Thermal effects on hysteresis for an $N=3$ square array of in-plane magnetized dots with the field applied along an array diagonal. The reduced inverse temperature is β. Thermal fluctuations cause the array ''shape'' anisotropy to decrease with increasing temperature. Interestingly, the minor loops disappear in favor of the central hysteresis loop with increasing temperature. For large temperatures no hysteresis is visible.

increasing temperature is to decrease array ''shape'' anisotropy. For large temperatures no hysteresis is visible.

At intermediate temperatures, the minor loops disappear in favor of the central hysteresis loop. This is because the hysteresis is controlled by nucleation of reversals at the array edges and corners. The corner dots, edge dots, and central dot experience different effective fields, and therefore have different thermal average values. This appears as different hysteresis shapes for different temperatures.

Reorientation transition

Reorientation transitions have been observed and predicted in fine particle and patterned array systems.[9,10] In the absence of other magnetic anisotropies, a planar array of magnetic dots will spontaneously align with moments in the array plane in order to minimize magnetostatic energies. One can expect then that a critical temperature exists for the in-plane ordering with a magnitude determined by the number, spacing, and size of the magnetic dots.

Such a transition is exhibited by an array of particles with individual anisotropies that favor alignment of each $\mathbf{m}_i$ perpendicular to the array plane. In order to describe this system, the anisotropy K of Eq. (2) is made positive with a value comparable to, but larger than, the magnetostatic energy $\mathbf{m}_i \cdot \mathbf{h}_{di}$. The equilibrium orientation of an array of dots is then calculated at different temperatures in zero field beginning at a high temperature, saturated state.

A useful quantity to examine is the specific heat at constant field C_H. This can be calculated from the internal energy U of the magnetic system by numerically evaluating $C_H = \partial U/\partial T$ with the applied field H_0 held constant.[11,12] The internal energy at finite temperatures is calculated according to:

$$U = -\frac{1}{2}\sum_i \langle \mathbf{m}_i \rangle \cdot \left(\mathbf{z}\frac{2K}{M}\langle m_{zi}\rangle + \langle \mathbf{d}_i \rangle \right), \qquad (6)$$

where i labels each magnetic dot.

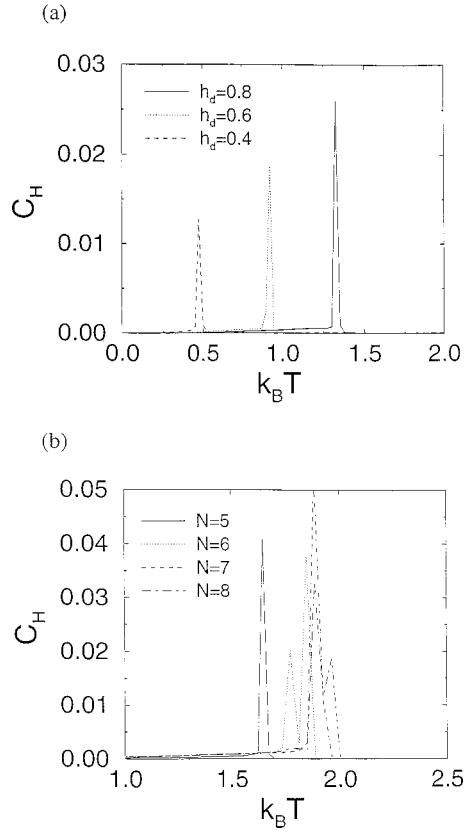

FIG. 7. Specific heat in a constant field ($H/M_0=1$) as a function of temperature for (a) different values of interdot coupling, and (b) different sizes of arrays. In (a) the array consists of 16 *perpendicularly* magnetized dots with uniaxial anisotropy $K/M_0=0.2$. The peak indicates a transition from perpendicular orientation to in plane, as the temperature is decreased. In (b) the interdot coupling is $h_d=1.0$.

Consider an array of dots with uniaxial anisotropy $K/M_0=0.2$. Suppose the array is initially prepared so that the magnetizations are all aligned perpendicular to the array plane at a temperature large enough to remove correlations due to dipolar coupling but low enough to avoid superparamagnetic behavior of the dots. With the positive anisotropy, the magnetizations of each dot will orient perpendicular to the array plane. As the temperature is lowered, dipolar fields become large enough to cause the dot moments to reorient in the array plane in order to reduce the total magnetostatic energy.

This transition appears in the specific heat as a sharp peak at the critical temperature. This is shown in Fig. 7(a) where C_H is plotted as a function of temperature for different values of interdot coupling. The array consists of 64 perpendicularly magnetized dots with uniaxial anisotropy $K/M_0=0.2$. The array has been cooled in zero applied field after saturation. The peak indicates a transition from perpendicular orientation to in plane. Note how the critical temperature of the reorientation transition increases linearly with the strength of the interaction h_d.

The effect of array size is shown in Fig. 7(b) where the specific heat at constant field is shown as a function of temperature for different sizes of arrays. The anisotropy is again $K/M_0=0.2$ and the array has been saturated perpendicular to the array plane and then cooled in zero applied field. The

critical temperature for reorientation into the array plane increases with array size N, but approaches a limiting value as N becomes very large. The interdot coupling is $h_d = 1.0$.

IV. SUMMARY AND CONCLUSIONS

A self-consistent mean-field calculation of field and temperature-dependent magnetization processes in arrays of small magnetic dots has been presented. Effects of array size and applied field orientation were investigated, and examples presented showing how details of the magnetization process depend on the geometry of the immediate neighborhood of magnetic dots in a two-dimensional array.

For small groups of weakly interacting dots, the shape of the array enters into the configuration energy of the array analogous to shape anisotropy effects in ferromagnets. The orientation of edge and corner magnets are most susceptible to applied fields and their relative to the external field determines the initiation of reversal mechanisms in the array. The shape of the array enters into the energy even when saturated for arbitrarily large arrays of regularly spaced dots, and may explain recently observed variations of magnetostatic excitations measured on submicron arrays of patterned magnetic dots.[3]

The strength of the interactions between magnetic particles depends on their size and spacing, and can drive reorientation transitions as a critical temperature is reached. Besides illustrating some features of weakly interacting arrays of single domain identical dots, these results have relevance to imperfect thin magnetic films and particle clusters which may display similar behaviors due to competitions between magnetocrystalline anisotropies and interparticle interactions.

The systems described in this paper were assumed to be finite but regular arrays of closely spaced magnetic dots. The results have relevance to ultrathin film films and two dimensional arrays of fine particles with distributions of sizes and spacing also. The reason is that the largest interparticle coupling contributions to the effective field of a small magnetic particle in a two dimensional array is due to the immediate neighborhood. Local order and symmetries will therefore be important for the magnetic properties of the system as a whole.

ACKNOWLEDGMENTS

This work was supported under ARO Grant No. DAAH04-94-G-0253. R.L.S. also acknowledges support under an ARC Small Grant, and NSF Grant Nos. INT-9603252 and DMR-9703783.

[1] E. C. Stoner and E. P. Wohlfarth, Philos. Trans. R. Soc. London, Ser. A **240**, 599 (1948).
[2] M. Hehn, K. Ounadjela, J. P. Bucher, F. Rousseaux, D. Decanini, B. Bartenlian, and C. Chappert, Science **272**, 1782 (1996).
[3] B. Hillebrands, C. Mathieu, M. Bauer, S. O. Demokritov, B. Bartenlian, C. Chappert, D. Decanini, F. Rousseaux, and F. Carcenac, J. Appl. Phys. **81**, 4993 (1997).
[4] R. L. Stamps and K. Ounadjela, in *Handbook of Nanostructured Materials and Nanotechnology*, edited by H. S. Nalwa (Academic, New York, 1999).
[5] R. L. Stamps and R. E. Camley, J. Magn. Magn. Mater. **177-181**, 813 (1998).
[6] R. L. Stamps and R. E. Camley, Phys. Rev. B (to be published).
[7] R. L. Stamps and B. Hillebrands, Appl. Phys. Lett. (to be published).
[8] R. E. Camley, Phys. Rev. B **56**, 2336 (1997).
[9] M. Hehn, K. Ounadjela, R. Ferre, W. Grange, and F. Rousseaux, Appl. Phys. Lett. **71**, 2833 (1997).
[10] A. B. MacIsaac, K. De'Bell, and J. P. Whitehead, Phys. Rev. Lett. **80**, 616 (1998).
[11] A. S. Carriço, R. E. Camley, and R. L. Stamps, Phys. Rev. B **50**, 13 453 (1994).
[12] R. E. Camley and R. L. Stamps, J. Phys.: Condens. Matter **5**, 3727 (1993).